THE ASTROPHYSICAL JOURNAL, 378:L17–L20, 1991 September 1

A COMPTON REFLECTION MODEL FOR THE COSMIC X-RAY AND GAMMA-RAY BACKGROUNDS

R. D. ROGERS[1] AND G. B. FIELD[2]
Harvard-Smithsonian Center for Astrophysics, 60 Garden Street, Cambridge, MA 02138
Received 1991 March 21; accepted 1991 June 12

ABSTRACT

We calculate the gamma-ray spectrum of an AGN in the Compton reflection model and consider the contribution of such sources to the cosmic gamma-ray background. The spectrum is composed of three parts: an X-ray power law, a broad hump from ≈ 10 to 120 keV due to reprocessing of the power-law X-ray spectrum by cold gas, and gamma rays which are due to the inverse-Compton scattering of X-rays.

We compute the contribution of such sources to the cosmic gamma-ray background and find that they provide an excellent fit to the entire background spectrum from 3 keV to 10 MeV. We derive constraints on the physical conditions in these sources based on our results and consider the possibility of observing such sources with GRO.

Subject headings: cosmic background radiation — gamma-rays: general — X-rays: sources

1. INTRODUCTION

The spectrum of the cosmic background radiation between 300 keV and 10 MeV was measured by a number of groups (see Rogers 1991b for references) including Trombka et al. (1978). It was found that the gamma-ray background (GRB) spectrum is approximately flat between 500 keV and 3 MeV, and then drops off as a power law with energy index ≈ 2 above 3 MeV. The origin of this feature, known as the "MeV bump," has not been determined, although a number of models have been put forward to explain it. These include both diffuse emission mechanisms (Brown & Stecker 1979; Olive & Silk 1985; Daly 1988) and models in which the integrated emission of point sources produces the background (Strong, Wolfendale, & Worral 1976; Bignami, Lichti, & Paul 1978; Grindlay 1978; Lichti, Bignami, & Paul 1978; Schönfelder 1978; Bignami et al. 1979; Mereghetti 1990).

In this *Letter*, we consider the possibility that both the GRB and the XRB are due to emission from AGN. In a previous paper (Rogers & Field 1991, hereafter RF) we have shown that the Compton reflection model of Fabian et al. (1990) can explain the entire 3–500 keV XRB. Here we extend our treatment of the Compton reflection process to gamma-ray energies and show that the resultant spectrum can simultaneously explain both the XRB and the GRB.

We calculate the entire 1 keV to 30 MeV spectrum of an AGN, then integrate the emission from an evolving population of such sources to find the intensity of the high-energy background. By fitting to the observed spectrum we derive constraints on the X- and gamma-ray emitting regions in these sources. Finally, we use our results to predict the number of sources which should be observable with the gamma-ray observatory satellite GRO. Throughout this *Letter* we assume a flat Friedmann-Robertson-Walker cosmology and take $H_0 = 50\ \mathrm{km\ s^{-1}\ Mpc^{-1}}$.

2. THE MODEL

In the calculation of our AGN spectrum we assume, as we did in RF, that the X-ray spectrum is a superposition of an initial power-law spectrum and a component which is reprocessed by Compton reflection from cold gas near the X-ray emitting region. The Compton-reflected spectrum, described in detail by several authors (RF; Guilbert & Rees 1988; Lightman & White 1988; White, Lightman, & Zdziarski 1988), is characterized by the photoelectric absorption of photons of energy less than ≈ 20 keV and by a steepening of the spectrum above ~ 120 keV, due to energy losses from repeated Compton scatterings. The resulting reflected spectrum exhibits a hump between 10 and 120 keV which, when redshifted by a factor of ~ 3, accounts for the break in the XRB spectrum at 40 keV.

The X-ray spectrum of an individual AGN is then a superposition of this reflected spectrum and the initial power-law spectrum. We parameterize the relative contributions of these two spectra in a single source by the parameter f, defined to be the ratio of the X-ray power incident on cold gas to the total power in the initial X-ray power-law spectrum. The resulting composite AGN spectrum with $f = 0.89$ and averaged over inclination angle is shown in Figure 1.

The gamma-ray spectrum of an AGN in the present model is comprised of two components as well. The first is simply the extension of the initial X-ray power-law spectrum to the gamma-ray regime. The second component is due to inverse-Compton scattering of X-rays by relativistic electrons as these photons leave the X-ray emitting region. If the initial X-ray power-law spectrum is due to inverse-Compton scattering of soft photons, then there must be relativistic electrons in the X-ray emitting region which will inverse-Compton scatter both the Compton-reflected X-rays and the initial power-law X-rays up to gamma-ray energies. The gamma-ray spectrum for a flat disk emitting region then depends on the Thomson depth, τ, and the energy distribution of the relativistic electrons.

We assume that the distribution of relativistic electron Lorentz factors, γ ($E \equiv \gamma m_e c^2$), is a power law which is cut off below γ_1, so that

$$\frac{dN_e}{d\gamma} = K_e \gamma^{-p}, \quad \gamma \geq \gamma_1, \tag{1a}$$

$$= 0, \qquad \gamma < \gamma_1, \tag{1b}$$

where p is the power-law index and K_e is a constant which

[1] Mail Stop 10.
[2] Mail Stop 51.

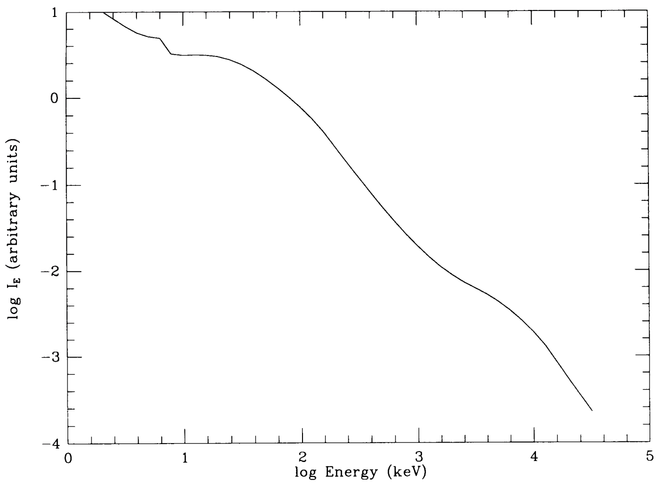

FIG. 1.—Composite Compton reflection-dominated AGN spectrum in the source rest frame, showing Compton-reflected component and second-order inverse-Compton gamma-ray component. Parameters are $\alpha = 1.1$, $f = 0.89$, $\tau = 0.002$, and $\gamma_1 = 28.0$.

normalizes the distribution to the total relativistic electron density, n_e. We discuss the reason for the cutoff in this distribution in § 4.

We assume that pair reprocessing is unimportant in the calculation of the spectrum. This is equivalent to the requirement that the compactness parameter, l, be small. Here

$$l \equiv \frac{L\sigma_T}{m_e c^3 \pi R} \tag{2}$$

where L is the total luminosity of the source, σ_T is the Thomson cross section, m_e is the electron mass, and R is the size of the emitting region. We will discuss this assumption later in this *Letter*. The gamma-ray spectrum can then be calculated from the relativistic inverse-Compton scattering emissivity (Blumenthal & Gould 1970). The number of photons of energy E produced by the scattering of a photon of energy ϵ is given by

$$\frac{dN_{\gamma,\epsilon}}{dt\,dE} = \frac{3\sigma_T c n(\epsilon) d\epsilon}{4\gamma^2 \epsilon} F(q, \Gamma)\,, \tag{3}$$

where $n(\epsilon)$ is the photon number density distribution incident on the scattering electron, and $F(q, \Gamma)$ is defined to be

$$F(q, \Gamma) \equiv \left[2q \ln q + (1 + 2q)(1 - q) + \frac{1}{2}\frac{(\Gamma q)^2}{1 + \Gamma q}(1 - q)\right], \tag{4}$$

where

$$\Gamma \equiv \frac{4\epsilon\gamma}{m_e c^2}\,, \tag{5}$$

$$q \equiv \frac{E/\gamma m_e c^2}{\Gamma(1 - E/\gamma m_e c^2)}\,. \tag{6}$$

Here $E \leq \gamma m_e c^2$, as required by energy conservation. When $\Gamma \ll 1$ the scattering is in the Thomson limit, while for $\Gamma \gg 1$ it is in the Klein-Nishina limit. We then integrate this expression over both the electron and initial photon distributions to get the gamma-ray spectrum. The number of photons emitted per unit volume in the emission region is then

$$\frac{dN}{dt\,dE\,dV} = \int_\gamma d\gamma \int_\epsilon \frac{dN_e}{d\gamma}\frac{dN_{\gamma,\epsilon}}{dt\,dE}\,. \tag{7}$$

The total high-energy spectrum ($E > 3$ keV) of an AGN is just the sum of the initial power law, the Compton-reflected X-ray spectrum and the inverse-Compton produced gamma-ray spectrum. If the spectral luminosity of the initial power-law X-ray emission as a function of energy E is given by L_E^0, then the observed spectral luminosity of an AGN is

$$L_E = L_E^0(1 - f) + L_E^0 f R_c(E) + \frac{E3K_e\sigma_T c V}{4}\int d\gamma\gamma^{-p-2}\int\frac{d\epsilon}{\epsilon}F(q, \Gamma)\int\frac{dy}{H}n(\epsilon, y) \tag{8}$$

where $R_c(E)$ is the effective reflectivity of the Compton reflection process, V and H are the volume and total height of the emitting region, and $n(\epsilon, y)$ is the number density of X-ray photons at height y above the disk. In equation (8), the first term gives the unreflected power-law luminosity, the second term gives the Compton-reflected component and the third term represents the second-order inverse Compton component. We assume that the emitting region is a disk of radius R and height H, with constant X-ray emissivity throughout. We also make the approximation that the density distribution at the center of the disk, multiplied by a correction factor, ζ, is representative of the whole disk. We have calculated ζ numerically and find that it is equal to 0.55 to within a few percent over the entire 3–1000 keV energy range (Rogers 1991b). The photon density averaged over z is then

$$\int\frac{dz}{H}n(\epsilon, z) = \frac{\zeta L_\epsilon^0 H^2}{\epsilon c V H}\left\{(f_\gamma + f - 2ff_\gamma)\left[1 - \ln\left(\frac{H}{R}\right)\right] + ff_\gamma R_c(\epsilon)\left[\frac{3}{2} - 2\ln\left(\frac{H}{R}\right)\right]\right\}. \tag{9}$$

Here f_γ is the fraction of the gamma-ray power which is not absorbed by cold gas. We take $f_\gamma \approx 0.4$ because the scattered gamma-ray distribution will be less anisotropic than the X-ray distribution. The complete expression for the spectral luminosity of a source is (Rogers 1991b)

$$L_E = L_E^0(1 - f) + L_E^0 f R_c(E) + E\zeta\frac{3}{4}\tau\frac{K_e}{n_e}\int d\gamma\gamma^{-p-2} \times \int\frac{d\epsilon}{\epsilon^2}F(q, \Gamma)L_\epsilon^0\left\{(f_\gamma + f - 2ff_\gamma) \times\left[1 - \ln\left(\frac{H}{R}\right)\right] + ff_\gamma R_c(\epsilon)\left[\frac{3}{2} - 2\ln\left(\frac{H}{R}\right)\right]\right\}. \tag{10}$$

The resulting composite spectrum is shown in Figure 1 for $\gamma_1 = 28$ and $\tau = 0.002$, so that $\approx$0.2% of the X-ray photons are inverse-Compton scattered into the gamma-ray band.

To compare our AGN spectrum with the observed XRB and GRB, we must include the redshift evolution of the source population. We assume, as we did in RF, that the comoving spectral volume emissivity is given by

$$\langle n_0 L_E\rangle = n_0 L_E(1 + z)^\beta \tag{11}$$

where n_0 and L_E are the number density of sources and the average spectral luminosity at the current epoch, respectively. Then the spectral intensity of the high-energy background is given by

$$I_E = \frac{3ct_0}{8\pi}\int n_0 L_{E(1+z)}(1 + z)^{-5/2+\beta}\,dz\,. \tag{12}$$

We have compared our model with the high-energy background by fitting for the values of the optical depth of the relativistic electron cloud, τ, and the elecron cutoff energy, γ_1, and using the XRB best-fit values derived in RF for the initial power-law spectral energy index, α, the covering factor, f, the evolution parameter, β, and the maximum redshift of emission, z_m. We have also found an overall best fit by optimizing the fit with respect to all six of these parameters simultaneously. Since the X-ray power-law spectrum is assumed to be due to inverse-Compton scattering of soft photons by the distribution of relativistic electrons, p is related to α by $p = 2\alpha + 1$ (e.g., Rybicki & Lightman 1979).

3. RESULTS

We find that our model provides a good fit to the data over the 3 keV to 10 MeV energy range. Figure 2 shows the high-energy background data (Trombka et al. 1977; Boldt 1987) and our best-fit model in which all parameters were allowed to vary. Note that the fit is excellent, with deviations less than a few percent per point, significantly smaller than the experimental errors. The model parameters for the fit shown in Figure 2 are $z_m = 4.6$, $\beta = 2.8$, $\alpha = 1.1$, and $f = 0.89$, with the additional gamma-ray parameters $\tau = 3 \times 10^{-4}$ and $\gamma_1 = 28$. The first four are essentially the same best-fit parameters derived by RF for the XRB alone. Fits using the XRB best-fit parameters derived in RF are also excellent. The GRB spectrum can then be qualitatively explained as the Compton-reflected X-ray spectrum shifted in energy to the gamma-ray regime by inverse-Compton scattering. The typical X-ray photon with energy between 2 and 10 keV will be inverse-Compton scattered by a typical electron with $\gamma_1 = 30$, to an energy in the range $(1–4)E\gamma_1^2 = 2–20$ MeV. The resulting gamma ray will then be redshifted by a factor of ≈ 4 to the energy range 0.5–5.0 MeV, the location of the MeV bump. The GRB power-law index of ≈ 2 above 3 MeV is due to the γ-dependence of the Klein-Nishina cross section at high energies.

As we did in RF, we have calculated a goodness-of-fit parameter, μ, roughly equal to the average percent deviation per point between model and data, and we have calculated constant μ-contours in the β-z_m plane. Requiring $\mu < 3$ results in the allowed parameter ranges given in Table 1. As discussed in RF, the large values of α we derive, 0.9–1.2, are consistent

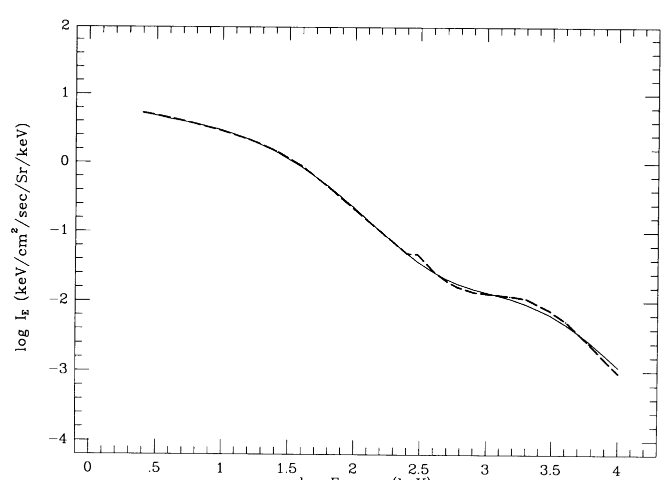

FIG. 2.—Best-fit model to high-energy background. Parameters are $z_m = 4.6$, $\beta = 2.8$, $\alpha = 1.1$, $f = 0.89$, $\tau = 3 \times 10^{-4}$, and $\gamma_1 = 28.0$.

TABLE 1

ALLOWED RANGES OF MODEL PARAMETERS

Parameter	Value	Parameter	Value
z_m	≥ 2.8	f	0.85–0.95
β	1.3–5.3	τ	$(3–10) \times 10^{-4}$
α	0.9–1.2	γ_1	15–30

with the canonical AGN spectral index of 0.7, due to the flattening of the spectrum with increasing energy. The result that the covering factor, f, is between 0.85 and 0.95, much greater than the geometrical covering of an accretion disk, can be explained if the primary X-ray power-law spectrum is due to inverse-Compton scattering of soft photons from a steady α-disk. In this case, the X-ray emission is anisotropic and is enhanced in the direction of the disk because of a relativistic kinematic effect, and may account for f as large as 0.88 (Ghisellini et al. 1990; Rogers 1991a). Finally, we find that the optical depth of the relativistic electron gas must be between 3×10^{-4} and 1×10^{-3} in order to correctly reproduce the relative GRB and XRB intensities, and that γ_1 must be in the range 15–30 to explain the shape and location of the MeV bump. In addition, it is possible to obtain reasonable fits when these parameters are distributed statistically with values which lie in the ranges given above.

4. DISCUSSION

As discussed previously, our model requires that the source compactness, l, be small, so that the probability for a typical gamma-ray to interact with an X-ray to produce an electron-positron pair is small. We have calculated this probability for a source with a flat disk geometry in which the emitting region scale height, H, satisfies $H/R \approx 0.01$, and find that as long as $l \leq 2$, then gamma rays of energy up to 30 MeV will not be absorbed on their way out of the source (Rogers 1991b). Such a compactness would be found for a source with luminosity, $L \approx 10^{44}$ ergs s^{-1}, and radius, $R \approx 3 \times 10^{14}$ cm, consistent with a model in which the XRB is produced by a population of AGNs, which have central masses of $\sim 10^8$ solar masses, radiate at 1% of their Eddington luminosities and have emission regions which extend to ~ 10 Schwarzschild radii. Their number density locally is then roughly equal to the Seyfert galaxy density (≈ 1% of L_* galaxies), but is ~ 50 times larger at $z \approx 3$. As has been pointed out by Daly (1991) this would imply that a significant fraction of L_* galaxies today should contain $10^8\ M_\odot$ black holes. Kormendy (1991) has recently shown that supermassive black holes do exist in the nuclei of many local galaxies, with masses averaging more than $10^8\ M_\odot$ per L_* of galaxy luminosity.

The origin of the low-energy cutoff in the electron distribution is more difficult to interpret. In the context of a magnetic corona, it could be associated with the acceleration of a typical electron in the corona, due to the conversion of magnetic field energy to electron kinetic energy during magnetic reconnection. Given the optical depth and scale height of the emission region, one can estimate the electron density, from

$$n_e = \frac{\tau}{\sigma_T H} \approx 2 \times 10^8 \text{ cm}^{-3}, \quad (13)$$

corresponding to an energy density in relativistic electrons

$$U_R = 2\gamma_1 n_e m_e c^2 = 10^4 \text{ ergs cm}^{-3} \quad (14)$$

so that the minimum magnetic field required to confine them is

$$B = (8\pi U_R)^{1/2} = 500 \text{ G}. \tag{15}$$

Although this field is large, it may be possible for an accretion disk to amplify a seed magnetic field to this magnitude. If a significant fraction of the magnetic energy is released in reconnection, it would be necessary for all electrons to attain $\gamma \geq \gamma_1$ to absorb it.

The presence of large magnetic fields implies that synchrotron radiation may be an important energy-loss mechanism. We can estimate the relative luminosities of synchrotron and inverse-Compton emission from the equation

$$\frac{P_S}{P_C} = \frac{B^2/8\pi}{2\sigma_{\rm SB}\, T^4/c} = 1.8 , \tag{16}$$

where $\sigma_{\rm SB}$ is the Stefan-Boltzmann constant, $B = 500$ G, and $T \approx 35{,}000$ K is the temperature of the accretion disk. We find that synchrotron self-absorption is important, reducing the ratio to ~ 1, so the synchrotron luminosity is important, but not dominant. We estimate that thermal emission will also be comparable to the X- and gamma-ray emission. Allowance for synchrotron and thermal energy increases the black hole masses and/or the number of AGNs required by a factor of ~ 3. This factor can be accommodated if every L_* galaxy typically has a black hole of mass $10^8\ M_\odot$, as recently demonstrated for local galaxies by Kormendy (1991).

We have used our model AGN spectrum to calculate the gamma-ray flux from a source in terms of its 2–10 keV flux. For each low-compactness AGN on the tentative GRO observing schedule (Kurfess 1991) we compare the predicted gamma-ray flux to the continuum sensitivity of the OSSE instrument (Kurfess et al. 1989) to determine whether OSSE will constrain its spectrum. Table 2 lists some of the sources which will be detected by OSSE. The highest energy for which spectral information will be obtained is also indicated. Since the model predicts that AGNs will have a steep spectrum (energy index ≈ 1.5–2.0) in the 150–800 keV range, it should be possible to determine whether our model is applicable to the sources in Table 2 which will be observed by OSSE above 300 keV. In addition, OSSE spectra at lower energies may constrain the contribution from Compton reflection in the rest of the sources listed in Table 2. We conclude that GRO will provide a useful test of this model.

TABLE 2

AGN TO BE OBSERVED BY OSSE

Name of AGN	Highest Observable Energy (keV)
NGC 4151	570
MGC 5-23-16	420
NGC 2992	410
3C111	280
MGC 8-11-11	260
ESO 141-55	260
NGC 3783	260
3C120	250

5. CONCLUSIONS

We have calculated the 3 keV to 30 MeV spectrum of an AGN in the Compton reflection model, assuming that the source compactness is low ($l \leq 2$) and that the primary X-rays are produced by the inverse-Compton scattering of soft photons by relativistic electrons. We have also assumed that the cold gas responsible for the Compton reflection process is contained in an accretion disk. In this model, the X-ray spectrum is a superposition of a power-law spectrum produced directly by the relativistic electrons, and a component which is reflected and reprocessed by the accretion disk. The gamma-ray spectrum is composed of two components as well: the extension of the original X-ray power-law to high energies, and the contribution of X-rays which have been inverse-Compton scattered into the gamma-ray regime on their way out of the source.

We have used these model AGN spectra to fit the spectrum of the cosmic background radiation from 3 keV to 10 MeV and find that the fits are excellent if a large fraction of the initial power-law X-ray luminosity is reprocessed by cold gas, the X-ray spectral index is ≈ 1, the optical depth, τ, for Compton scattering in the emission region is $\approx 3 \times 10^{-4}$, and if the relativistic electron distribution is cut off below $\gamma_1 \approx 28$.

We have used our fit results to derive constraints on the physical properties of such sources if they dominate the high-energy background. We have also calculated the numbers of such sources which should be observable by GRO.

This work was supported in part by NASA grant NAGW-931.

REFERENCES

Bignami, G. F., Fichtel, C. E., Hartman, R. C., & Thompson, D. J. 1979, ApJ, 232, 649
Bignami, G. F., Lichti, G. G., & Paul, J. A. 1978, A&A, 68, L15
Blumenthal, G. R., & Gould, R. J. 1970, Rev. Mod. Phys., 42, No. 2, 237
Boldt, E. 1987, Phys. Rept., 146, No. 4, 215
Brown, R. W., & Stecker, F. W. 1979, Phys. Rev. Letters, 43, 315
Daly, R. A. 1988, ApJ, 324, L47
———. 1991, preprint
Fabian, A. C., George, I. M., Miyoshi, S., & Rees, M. J. 1990, MNRAS, 242, 14p
Ghisellini, G., George, I. M., Fabian, A. C., & Done, C. 1990, MNRAS, 248, 14
Grindlay, J. E. 1978, Nature, 273, 211
Guilbert, P. W., & Rees, M. J. 1988, MNRAS, 233, 475
Kormendy, J. 1991, BAAS, 23, 937
Kurfess, J. D. 1991, private communication
Kurfess, J. D., et al. 1989, in Proc. Gamma Ray Observatory Science Workshop, ed. W. N. Johnson (Greenbelt: NASA/Goddard Space Flight Center), 3
Lichti, G. G., Bignami, G. F., & Paul, J. A. 1978, Ap. Space Sci., 56, 403
Lightman, A. P., & White, T. R. 1988, ApJ, 335, 57
Mereghetti, S. 1990, ApJ, 354, 58
Olive, K. A., & Silk, J. 1985, Phys. Rev. Letters, 55, 2362
Pounds, K. A., Nandra, K. A., Stewart, G. C., George, I. M., & Fabian, A. C. 1990, Nature, 344, 132
Rogers, R. D. 1991a, ApJ, submitted
———. 1991b, Ph.D. thesis, Harvard University
Rogers, R. D., & Field, G. B. 1991, ApJ, 370, L57 (RF)
Rybicki, G. B., & Lightman, A. P. 1979, Radiative Processes in Astrophysics (New York: Wiley)
Schönfelder, V. 1978, Nature, 275, 719
Strong, A. W., Wolfendale, A. W., & Worral, D. M. 1976, MNRAS, 175, 23p
Trombka, J. I., et al. 1977, ApJ, 212, 925
White, T. R., Lightman, A. P., & Zdziarski, A. A. 1988, ApJ, 331, 939